

# Spatially resolved isotopic analysis of a uranium-bearing particle from inside the Fukushima Daiichi unit 2 reactor using high-resolution SIMS

Received: 6 November 2025

Accepted: 16 February 2026

Published online: 19 February 2026

Cite this article as: Yoshida T., Maeda K., Sekio Y. *et al.* Spatially resolved isotopic analysis of a uranium-bearing particle from inside the Fukushima Daiichi unit 2 reactor using high-resolution SIMS. *Sci Rep* (2026). <https://doi.org/10.1038/s41598-026-40875-y>

Takeru Yoshida, Koji Maeda, Yoshihiro Sekio, Hideki Tomita, Yoshihiro Iwata, Mutsumi Hirai, Masato Mizokami & Tetsuo Sakamoto

We are providing an unedited version of this manuscript to give early access to its findings. Before final publication, the manuscript will undergo further editing. Please note there may be errors present which affect the content, and all legal disclaimers apply.

If this paper is publishing under a Transparent Peer Review model then Peer Review reports will publish with the final article.

ARTICLE IN PRESS

**Title**

Spatially Resolved Isotopic Analysis of a Uranium-Bearing Particle from Inside the Fukushima Daiichi Unit 2 Reactor Using High-Resolution SIMS

**Authors**

Takeru Yoshida<sup>1, 2</sup>, Koji Maeda<sup>2</sup>, Yoshihiro Sekio<sup>2</sup>, Hideki Tomita<sup>3</sup>, Yoshihiro Iwata<sup>4</sup>, Mutsumi Hirai<sup>5</sup>, Masato Mizokami<sup>5</sup>, Tetsuo Sakamoto<sup>1\*</sup>

**Affiliations**

<sup>1</sup>Electrical Engineering and Electronics Program, Graduate School of Engineering, Kogakuin University, Hachioji-shi, Tokyo 192-0015, Japan

<sup>2</sup>Oarai Nuclear Engineering Institute, Japan Atomic Energy Agency, Oarai-machi, Ibaraki 311-1393, Japan

<sup>3</sup>Department of Applied Energy, Nagoya University, Chikusa-ku, Nagoya 464-8603, Japan

<sup>4</sup>CLADS, Japan Atomic Energy Agency, Tokai-mura, Ibaraki 319-1195, Japan

<sup>5</sup>Tokyo Electric Power Company Holdings, Inc., Chiyoda-ku, Tokyo 100-8560, Japan

\*Correspondence and requests for materials should be addressed to Tetsuo Sakamoto (email: ct13087@ns.kogakuin.ac.jp).

**Text****Summary**

Characterizing fuel debris (FD) is critical for decommissioning the Fukushima Daiichi Nuclear Power Station (FDNPS). Samples collected from inside the reactor building through various methods provide valuable insights into the properties of FD. However, localized isotope data from these samples have not been previously reported.

In this study, we present the first global report of isotope imaging and ratio data for the FDNPS particle obtained using our novel high-spatial-resolution secondary ion mass spectrometry (SIMS) technique developed for FD analysis. The method successfully mapped the spatial distributions of uranium, a key nuclear fuel component, and boron- $^{10}$  ( $^{10}\text{B}$ ), a control rod material, within the particle.

In addition, the spatial distributions and isotope ratios of B and lithium (Li) in the particles provide definitive evidence that  $^{10}\text{B}$  ( $n, \alpha$ )  $^7\text{Li}$  reactions occur in the control rod during normal reactor operation. These findings provide new insights into the FD composition and underscore the effectiveness of SIMS for the detailed characterization of FD.

**Main**

The 2011 Great East Japan Earthquake and subsequent tsunami triggered severe accidents at the Fukushima Daiichi Nuclear Power Station (FDNPS), operated by Tokyo Electric Power Company Holdings, Inc., including core meltdowns and explosions in reactor buildings<sup>1,2</sup>. The removal of FD is a critical challenge in the ongoing decommissioning of FDNPS. This FD consists of solidified materials formed when the reactor's nuclear fuel melted and reacted at high temperatures with surrounding structural components such as metal materials and concrete. The complete extent and composition of the debris remain largely unknown. Safe, systematic removal requires a comprehensive understanding of three key factors: (i) FD characteristics and spatial distribution, (ii) core meltdown progression, and (iii) fission product behavior. Effective removal strategies depend on this foundational knowledge base.

Since the accident, extensive efforts have been made to characterize the FD. In 2012, remotely operated robotic systems were deployed to investigate the interior of the primary containment vessel, progressively revealing the internal conditions<sup>3</sup>. These operations enabled the collection of a limited number of samples from inside the reactor buildings. These samples are currently undergoing analysis at

a radioactive materials facility in Ibaraki Prefecture using advanced characterization techniques, including scanning electron microscopy with energy-dispersive X-ray spectroscopy and wavelength-dispersive X-ray spectroscopy, transmission electron microscopy, and inductively coupled plasma mass spectrometry (ICP-MS)<sup>4, 5</sup>. The findings from these analyses are used to evaluate the characteristics of the FD across the reactor units. However, current studies on FDNPS samples lack detailed insights into the local-scale distribution of isotope elements and their respective isotope ratios, a significant knowledge gap that must be addressed.

Comprehensive FD characterization requires detailed information on the isotope ratios of constituent elements, which are critical indicators for safety assessments. For instance, evaluating the safety of FD retrieval and storage necessitates confirming the absence of criticality risk. To this end, the isotope ratios of boron (B), a neutron-absorbing element used as B<sub>4</sub>C control rods in the FDNPS reactor, and uranium (U), the nuclear fuel, are essential. The isotopic compositions of B and U in FDNPS samples have been primarily analyzed using ICP-MS<sup>4,5</sup>. However, this technique requires chemical pretreatment, which eliminates spatial distribution data and provides only the average elemental concentrations. Given the heterogeneous and localized distribution of elemental components in FD, disregarding spatially resolved isotopic information can result in an incomplete analysis.

Secondary ion mass spectrometry (SIMS) offers unique capabilities for nuclear material characterization, enabling direct analysis of solid samples without pretreatment while providing isotope and spatial distribution data. This technique has proven to be valuable for studying fission product distribution, fuel pellet burnup<sup>6,7</sup>, and analyzing environmental samples from FDNPS<sup>8,9,10</sup>. Despite its demonstrated potential for FD analysis, SIMS has not yet been applied to samples collected directly from FDNPS reactor buildings. In addition, although some commercially available SIMS instruments can achieve micrometer- or sub-micrometer-scale spatial resolution, it is generally difficult to analyze the interior of a small particle because any sectioning method is integrated.

This study employs a high spatial resolution SIMS system developed by Sakamoto et al. at the Japan Atomic Energy Agency Oarai Nuclear Engineering Institute, a facility dedicated to the treatment of radioactive materials<sup>11</sup>. The system was designed to enable high-resolution SIMS analysis of both surface and interior of

small debris by employing a focused ion beam (FIB) as a SIMS primary beam and a cross-sectioning tool. This advanced SIMS system enables the simultaneous observation of surface morphology, visualization of internal structure, compositional imaging, and isotope analysis of microscale sample regions<sup>12</sup>. These integrated capabilities enable three-dimensional structural and isotopic characterization of both surface and interior regions at microscopic scales, a significant advancement over conventional SIMS approaches in terms of practical spatial resolution and multifunctional analysis for radioactive samples.

The novel high-resolution SIMS system demonstrates strong potential for analyzing minimal quantities of FD from preliminary retrieval operations. We applied SIMS analysis to a U-bearing particle collected from the FDNPS Unit 2 reactor, establishing the first reported localized isotopic analysis of the FDNPS sample using advanced SIMS methodology. These findings validate the effectiveness of the proposed method for detailed FD characterization.

## Results

### Secondary electron imaging using FIB

Figure 1 shows secondary electron images of a particle collected in the FDNPS reactor building obtained using the SIMS-integrated focused ion beam (FIB) system. Approximately half of the particle surface area is embedded in the indium foil for sample preparation. The images reveal a nearly spherical morphology with a diameter of approximately 50  $\mu\text{m}$ .

To investigate the internal structure of the particle, cross-sectional milling was performed using FIB. Figures 1(b)–1(d) show the progressive slicing of the particle from the outer surface toward the center. The cross-sections reveal some parallel streaks aligned with the direction of the incident ion, which are likely to be FIB milling artifacts. In addition, no significant bubbles or voids were observed in either the surface or interior regions.

The absence of internal bubbles provides valuable insight into the thermal conditions during particle formation. If particles solidified at high temperatures or underwent rapid cooling, volatile components were likely expelled early, preventing bubble formation. Alternatively, solidification at lower temperatures, with reduced vapor pressure of the volatile substance, may have inhibited bubble formation. In either scenario, the evaporation or absence of volatiles during solidification likely contributed to the compact structure of the particle.

Conventional analytical techniques, such as SEM-EDS, can

resolve the spatial features of individual particles; however, achieving optimal spatial resolution often requires additional surface treatments after FIB cross-sectioning, which can complicate repeated analysis of internal structures, particularly for radioactive samples. Moreover, such approaches are not well suited for successive FIB milling and analysis while preserving consistent spatial resolution across multiple layers. In contrast, the high spatial resolution SIMS enables direct compositional and isotopic analysis of freshly FIB-milled surfaces without additional surface treatment, allowing repeated FIB sectioning and analysis while maintaining spatial resolution. This capability enables precise internal structural characterization and subsequent compositional interpretation, representing a critical advancement for FD analysis.

### **SIMS compositional imaging**

Figure 2 shows the SIMS compositional imaging of particle cross-sections at various stages of FIB processing. In the pre-FIB images (Figs. 2(a-1) and 2(a-5)), Al, Fe, and Zr, as well as faint traces of  $\text{UO}_2$ , were distributed across the particle surface. As FIB processing penetrated deeper, additional elements, including Cr and more prominent  $\text{UO}_2$ , were detected along the surface elements. In contrast, Al was absent in the cross-section regions, indicating its confinement to the particle surface.

The presence of Zr and  $\text{UO}_2$  in the interior likely originates from zircaloy cladding tubes and sintered uranium dioxide, respectively. Fuel particles formed within the FDNPS reactor building are classified into two types: Type I, formed via a melting–solidification process, and Type II, formed through an evaporation–condensation process. This classification is based on zirconium content, as Zr and  $\text{ZrO}_2$  exhibit considerably lower volatility than other oxides<sup>13</sup>. The particle analyzed in this study, which contains substantial Zr, is categorized as Type I, indicating formation through melting and subsequent solidification. This interpretation aligns with the secondary electron imaging observations of particle morphology and size.

The Fe and Cr detected within the particle likely originated from the structural components of the reactor, such as carbon steel and stainless steel. The presence of U, Zr, Fe, and Cr in a single particle indicates that molten fuel rod materials mixed with structural steel during particle formation. The Al detected on the surface is probably derived from thermal shielding materials beneath the reactor pressure vessel or paints used in the reactor building. The absence of Al in the

particle indicates a multistage formation process: initial melting and solidification of the fuel and structural materials, followed by surface deposition of Al from environmental sources after formation.

Figure 3 shows detailed SIMS compositional imaging of the particle after FIB-based cross-section processing. This analysis reveals the spatial distributions of Li, B, Cr, Fe, Zr, and U within the particle. The overlapping distributions of these elements indicate a complex mixture of particles comprising three distinct regions, each separated by a few micrometers: a U-Zr coexistent region (Fig. 3d), the Fe-B-Li coexistent region (Figs. 3h and 3k), and a Cr-only region, where Cr appears without overlapping other detected elements (Fig. 3g is compared with other panels in Fig. 3). The lack of spatial overlap between Cr and Fe, despite their common origin, may reflect differences in their oxidation behaviors and chemical reactivities under severe accident conditions, resulting in phase separation during melt-solidification. The U-Zr coexistent region indicates a spatial association between U and Zr at the micrometer scale. Such an association is consistent with the formation of U-Zr-O phases reported in previous TEM studies of FDNPS samples, although direct crystallographic confirmation was not performed for the present particle<sup>5,13</sup>. Among these, the presence of B is noteworthy. Understanding core meltdown progression at the FDNPS requires investigating high-temperature interactions among reactor components, such as UO<sub>2</sub> (fuel pellets), Zircaloy (cladding and channel box), B<sub>4</sub>C (control rods), and other structural materials<sup>14,15,16</sup>. Previous studies have highlighted the significance of B<sub>4</sub>C reactions with surrounding materials, particularly because FDNPS reactors that have experienced severe accidents uniquely used B<sub>4</sub>C as a control rod material. The SIMS imaging data presented here represent the world's first compositional imaging of mixed melt-solidification products from reactor core components, including B<sub>4</sub>C constituent distributions. These findings provide critical validation data for previous experimental and simulation studies of high-temperature reactor material interactions.

Furthermore, SIMS imaging reveals a significant spatial relationship between B and U, which is critical for criticality safety management (Fig. 3l). To date, no analysis of FDNPS samples has confirmed the distribution of U and B. This new evidence provides valuable insight into the characteristics of FD. The data show that U is distributed throughout the particle, whereas B is more concentrated near the periphery. Because of their relative freezing points, U, with

a lower freezing point than B, likely solidified earlier during cooling, leading to its central distribution. In contrast, B migrated outward and concentrated near the surface.

Although this explanation does not account for all factors, such as the chemical states of elements, a more comprehensive analysis is necessary to fully elucidate the particle formation process. Nevertheless, this study enables microscale analysis of the localized distribution behavior of B and other components. This capability, enabled by the high spatial resolution of SIMS with in-situ cross-sectioning feature, represents a considerable advancement in the characterization of complex FD materials.

### **SIMS Isotope ratio analysis**

Figure 4(d) shows the U isotope ratio analysis of the particle cross-section described in the previous section. The weight ratio ( $^{235}\text{U}/^{235}\text{U}+^{238}\text{U}$ ) was calculated as  $2.51 \pm 0.102$  wt% based on the integrated peak intensities of  $^{235}\text{U}$  and  $^{238}\text{U}$ . This value is considerably higher than the natural U isotope ratio (0.72 at%)<sup>17</sup> but lower than the average enrichment level of 3.8 wt% used during the initial fuel loading of Unit 2<sup>18</sup>. These findings indicate that the U detected in the particle likely originated from fuel that had undergone partial burnup during reactor operation. This interpretation is consistent with previously reported ICP-MS analyses of U isotopic ratios for samples collected from various locations within Unit 2, where the measured  $^{235}\text{U}$  enrichment values span a range that includes the value obtained in this study<sup>13</sup>.

Following the FDNPS accident, it is considered that the fuel and structural materials were melted and mixed, then possibly resulted in FD containing uranium macroscopically homogeneous, but microscopically inhomogeneous. Conventional isotope ratio analysis methods, such as ICP-MS, require sample dissolution, which provides only bulk-averaged isotope ratios and thus cannot resolve such microscopic inhomogeneous. In contrast, this study directly determined U isotope ratios from individual particles, demonstrating the potential for more precise burnup evaluations and enhanced understanding of sample formation processes in future analyses of FDNPS materials.

Figures 3(i), 3(j), and 3(k) show the spatial distribution of  $^7\text{Li}$  and  $^{10}\text{B}$  within the particle cross-section. The co-localization of these nuclides suggests a possible relationship.  $^{10}\text{B}$ , used in the control rods at FDNPS, captures neutrons to generate  $^7\text{Li}$  via the  $^{10}\text{B}(n, \alpha)^7\text{Li}$

reaction<sup>19</sup>. The detection of  $^{10}\text{B}$  and  $^7\text{Li}$  at the same location provides strong evidence of neutron capture within the particle during normal reactor operation.

If the detected  $^7\text{Li}$  was produced via the  $^{10}\text{B} (n, \alpha) ^7\text{Li}$  reaction, its isotope ratio should differ from the natural abundance. Figures 4(e) and 4(f) show the measured isotope ratios of B and Li within the particle. The  $^{11}\text{B}/^{10}\text{B}$  ratio was  $(4.37 (\pm 0.140))$ , slightly higher than the natural value of  $(4.02)^{17}$ , whereas the  $^7\text{Li}/^6\text{Li}$  ratio was  $(66 (\pm 12))$ , substantially exceeding the natural ratio of  $(12.2)^{17}$ . These results are consistent with the expected nuclear reaction behavior, where neutron absorption reduces  $^{10}\text{B}$  abundance and increases  $^7\text{Li}$  abundance. This finding confirms that the SIMS compositional imaging captured the history of the  $^{10}\text{B} (n, \alpha) ^7\text{Li}$  reaction during normal reactor operation, representing the first imaging-based evidence of this process. During normal FDNPS operation,  $\text{B}_4\text{C}$  control rods are inserted from the bottom of the core between fuel assemblies to regulate U fuel criticality. However, some regions absorb neutrons while others do not because the control rods are not fully inserted throughout the reactor core, even during active operation. Therefore, the origin of the control rod materials detected in FDNPS-derived samples can be more accurately inferred by analyzing the history of the  $^{10}\text{B} (n, \alpha) ^7\text{Li}$  reaction, as demonstrated in this study.

Although imaging data have not been published, Fueda et al. previously reported that cesium-bearing radioactive particles released into the environment from the FDNPP underwent the  $^{10}\text{B} (n, \alpha) ^7\text{Li}$  reaction<sup>20</sup>. These particles were likely formed through an evaporation–condensation mechanism, distinct from the melting–solidification process of the particle examined in this study. Although the  $^{11}\text{B}/^{10}\text{B}$  isotope ratio reported by Fueda et al. was approximately consistent with our findings, their measured  $^7\text{Li}/^6\text{Li}$  was an order of magnitude higher. This discrepancy in the Li isotopic ratio may be attributed to the preferential uptake of Li during particle formation or to Li volatilization, as discussed by Fueda et al.<sup>20</sup>

For particles formed via evaporation–condensation processes, B and Li may exhibit distinct spatial distributions despite coexisting in the same particle. Therefore, combining the isotopic ratio analysis of Li with the spatial distributions of both B and Li elements could provide a unique indicator for identifying the mechanisms of particle formation.

## Discussion

This study demonstrates the effectiveness of high-resolution SIMS for FD characterization by analyzing a U-bearing particle collected from the FDNPS Unit 2 reactor. The analytical results obtained are presented herein.

Through iterative cross-sectional analysis coupled with compositional imaging, distinct compositional structures between the particle's surface and interior regions were identified. The spatial distribution of elements indicates that nuclear fuel, reactor structural materials, and control rod components were formed via the melting-solidification process at micrometer scales.

This high-resolution compositional analysis not only enhances our understanding of the sample's formation process but also provides the first confirmed evidence of nuclear fuel and control rod materials coexisting within a single particle. The signature of the  $^{10}\text{B} (n, \alpha) ^7\text{Li}$  reaction was also revealed, confirming that the control rod material embedded in the particle absorbed neutrons during normal reactor operation.

The previously underexplored B-Li correlation offers a promising novel indicator for tracing particle origins and formation history through isotope ratios, spatial distributions, and nuclear reaction signatures.

These unprecedented insights underscore the unique value of high-resolution SIMS for FDNPS FD analysis. Future work will integrate this approach with traditional analytical methods to enable comprehensive, multidimensional characterization of Unit 2 FD<sup>21,22</sup>, demonstrating its broader applicability.

## Methods

### Sample collection and preparation

The sample was collected in February 2017 by wiping smears from a robot that had accessed the interior of the primary containment vessel of Unit 2 at the FDNPS<sup>23</sup>. These smears likely originated from sediments deposited along the path of the control rod drive replacement rail along the robot. Upon acceptance, the radioactivity of the sample was evaluated by measuring the ambient dose equivalent rate at the surface of the sealed sample container, yielding a value of approximately 2000  $\mu\text{Sv/h}$ . For SIMS analysis, the collected sample was gently pressed onto indium foil (99.99% purity, Nilaco Corp.) and mounted on the SIMS apparatus stage. A target particle was selected by observing the secondary electron images using the FIB system integrated with the SIMS instrument.

### **Secondary ion mass spectrometry**

Isotope analysis of the target particles was performed using a time-of-flight (TOF) SIMS system. The SIMS instrument used in this study was a custom-built device developed by Tetsuo Sakamoto. It uses a Ga<sup>+</sup> ion beam generated from the integrated FIB system, operating at an acceleration voltage of 30 kV, which functions both as a preanalysis tool for sample processing and as the primary probe for secondary ion generation. The spatial resolution of ion imaging achieved with this system has been reported to be on the order of ~40 nm<sup>12</sup>. To minimize radiation-induced noise during the analysis of highly radioactive materials, the detector was enclosed in a lead shield.

To visualize the internal composition of the particle, sequential cross-section milling and compositional imaging were performed using a Ga<sup>+</sup> ion beam with a DC current of 1.8 nA. Cross-section milling was carried out in DC mode. Subsequent SIMS imaging was conducted via raster scanning with the same DC ion beam operated in pulsed mode at a repetition rate of 10 kHz and a pulse width of 200 ns. For overview imaging, the scanning field of view was 60 μm with a resolution of 256 x 256 pixels, delivering 50 pulses per pixel. For the final cross-sectional compositional imaging, the field of view was adjusted to 40 μm, with 500 pulses per pixel to enhance image resolution.

The isotope ratio was calculated using the integrated intensity of mass spectral peaks detected within the cross-sectioned region of the particle. To ensure reliability, the mass spectra were acquired five times, and the average value and standard deviation ( $\pm\sigma$ ) were used to evaluate the isotope ratio. The TOF-MS system enables the simultaneous detection of all secondary ions without limiting the measurable mass range.

Integrated peak intensities were obtained by summing the total counts within predefined m/z windows corresponding to each isotope peak. Peak fitting was not applied; instead, a fixed mass window approach was used to ensure consistent treatment across repeated measurements.

Mass calibration of the TOF-MS system was performed by assigning the flight-time axis using the Ga<sup>+</sup> peak originating from the FIB ion source and the In<sup>+</sup> peak from the indium foil as reference masses.

Isotopic ratios were derived from the integrated peak intensities without the use of external standards during the present

measurements. The reliability of the SIMS-based isotope ratio analysis for boron has been previously evaluated using samples with different  $^{10}\text{B}/^{11}\text{B}$  enrichment levels, confirming the reproducibility of the method. For uranium, although no external calibration was applied in this study, the same SIMS system has been independently validated in separate experiments using uranium samples with known isotopic compositions. Lithium isotope ratios were evaluated qualitatively due to the limited signal intensity.

No explicit correction for instrumental mass bias was applied. Since the isotope ratios evaluated in this study involve isotopes of the same element with small mass differences, the influence of mass bias on the relative isotope ratios is considered to be limited.

The detection limits of SIMS are known to depend strongly on the element, matrix composition, and measurement conditions. In the present study, absolute detection limits were not determined using standard reference materials, as the primary objective was spatially resolved isotopic analysis rather than quantitative elemental determination. However, the successful acquisition of isotope ratio data with adequate counting statistics for isotope ratio evaluation for U, B, and Li indicates that their concentrations in the analyzed regions were above the effective detection limits under the present analytical conditions.

## References

- [1] Tanaka, S. Accident at the Fukushima Daiichi nuclear power stations of TEPCO -outline & lessons learned-. *Proc. Jpn. Acad., Ser. B.* **88**, 471-484 (2012).
- [2] Tokyo Electric Power Corporation. Fukushima nuclear accident analysis report. [https://www4.tepco.co.jp/en/press/corp-com/release/betu12\\_e/images/120620e0104.pdf](https://www4.tepco.co.jp/en/press/corp-com/release/betu12_e/images/120620e0104.pdf)
- [3] Tokyo Electric Power Corporation. The status of fuel debris retrieval. <https://www.tepco.co.jp/en/hd/decommission/progress/retrieval/index-e.html>
- [4] Japan Atomic Energy Agency. Debris wiki. <https://fdada-plus.info>
- [5] Kurata, M., Okuzumi, N., Nakayoshi, A., Ikeuchi, H. & Koyama, S. Step-by-step challenge of debris characterization for the decommissioning of Fukushima Daiichi nuclear power station (FDNPS). *J. Nucl. Sci. Technol.* **59**, 807-834 (2022)
- [6] C. T. Walker. et al. SIMS analysis of an UO<sub>2</sub> fuel irradiated at low temperature to 65 MWd/kgHM. *J. Nucl. Mater.* **393**, 212-223 (2009).

- [7] S. Portier., S. Brémier., C.T. Walker. Secondary ion mass spectrometry of irradiated nuclear fuel and cladding: An overview. *Int. J. Mass Spectrom.* **263**, 113-126 (2007).
- [8] Martin, P. G. et al. Provenance of uranium particulate contained within Fukushima Daiichi nuclear power plant unit 1 ejecta material. *Nat. Commun.* **10**, 2801 (2019).
- [9] Kurihara, E. et al. Particulate plutonium released from the Fukushima Daiichi meltdowns. *Sci. Total Environ.* **743**, 140539 (2020).
- [10] Sakamoto, T. et al. Isotope-selective microscale imaging of radioactive Cs without isobaric interferences using sputtered neutral mass spectrometry with two-step resonant ionization employing newly-developed Ti:Sapphire lasers. *Anal. Sci.* **34**, 1265-1270 (2018).
- [11] Sakamoto, T. et al. Establishment of characterization method for small fuel debris using the world's first isotope micro imaging apparatus. JAEA-Review 2024-005.
- [12] Sakamoto, T., Koizumi, M., Kawasaki, J., Yamaguchi, J. Development of a high lateral resolution TOF-SIMS apparatus for single particle analysis. *Appl. Surf. Sci.* **255**, 3406-3412 (2008).
- [13] Tokyo Electric Power Corporation. Sample analysis to determine accident progression. [https://www.tepco.co.jp/en/hd/decommission/information/accident\\_unconfirmed/pdf/221110e0106.pdf](https://www.tepco.co.jp/en/hd/decommission/information/accident_unconfirmed/pdf/221110e0106.pdf)
- [14] Sumita, T., Kobata, M., Takano, M. & Ikeda-Ohno, A. High temperature reaction of multiple eutectic-component system: the case of solid metallic Zr and molten stainless steel-B<sub>4</sub>C. *Materialia*. **20**, 101197 (2021).
- [15] Sumita, T., Kitagaki, T., Takano, M. & Ikeda-Ohno, A. Solidification and re-melting mechanisms of SUS-B<sub>4</sub>C eutectic mixture. *J. Nucl. Mater.* **543**, 152527 (2020).
- [16] Steinbrück, M. Influence of boron carbide on core degradation during severe accidents in LWRs. *Ann. Nucl. Energy.* **64**, 43-49 (2014).
- [17] Coursey, J. S., Schwab, D. J., Tsai, J. J. & Dragoset, R. A. Atomic weights and isotopic compositions (version 4.1). *NIST Physical Measurement Laboratory*. (2015).
- [18] Tokyo Electric Power Corporation. Plant specifications. <https://fdada.info/docs/pdf/PS-Unit2-01.pdf>
- [19] Iwamoto, O. et al. Japanese evaluated nuclear data library version 5: JENDL-5. *J. Nucl. Sci. Technol.* **60**, 1-60 (2023).
- [20] Fueda, K. et al. Volatilization of B<sub>4</sub>C control rods in Fukushima Daiichi nuclear reactors during meltdown: B-Li isotopic signatures in

- cesium-rich microparticles. *J. Hazard. Mater.* **428**, 128214 (2022)
- [21] Tokyo Electric Power Corporation. Fukushima Daiichi nuclear power station unit 2 PCV internal investigation/ status of fuel debris trial retrieval. [https://www.tepco.co.jp/en/hd/decommission/information/newsrelease/reference/pdf/2024/reference\\_20241128\\_03-e.pdf](https://www.tepco.co.jp/en/hd/decommission/information/newsrelease/reference/pdf/2024/reference_20241128_03-e.pdf)
- [22] Tokyo Electric Power Corporation. Fukushima Daiichi nuclear power station unit 2 PCV internal investigation/ status of fuel debris trial retrieval. [https://www.tepco.co.jp/en/hd/decommission/information/newsrelease/reference/pdf/2025/reference\\_20250424\\_02-e.pdf](https://www.tepco.co.jp/en/hd/decommission/information/newsrelease/reference/pdf/2025/reference_20250424_02-e.pdf)
- [23] Tokyo Electric Power Corporation. Regarding the status of investigations, sampling and analysis of the interior of the nuclear reactor containment vessel. [https://www.tepco.co.jp/decommission/information/committee/local\\_reconciliation/pdf/2018/1180823\\_05-j.pdf](https://www.tepco.co.jp/decommission/information/committee/local_reconciliation/pdf/2018/1180823_05-j.pdf)

### **Acknowledgements and Funding Information**

This work was supported by the JAEA Nuclear Energy S&T and Human Resource Development Project through concentrating wisdom (Grant Number JPJA21P21465814). The authors would like to thank Enago ([www.enago.jp](http://www.enago.jp)) for the English language review.

The authors wish to acknowledge the contributions of Dr. Masabumi Miyabe, who contributed to validation of the obtained data and passed away before the completion of this manuscript.

### **Author Contributions**

T.Y. carried out the investigation, performed formal analysis, prepared visualizations, and wrote the original draft of the manuscript. T.S. developed the methodology and supervised the overall project. K.M. and Y.S. were responsible for funding acquisition, provided resources, contributed to validation of part of the data, and assisted with writing - review and editing. H.T. and Y.I. contributed to validation of the obtained data. M.H. and M.M. provided the analysis samples and contributed to validation and critical review of the manuscript. All authors discussed the results and approved the final version of the manuscript.

### **Competing interest**

The authors declare no competing interests.

**Data availability**

The data that support the findings of this study were obtained from samples provided by Tokyo Electric Power Company Holdings, Inc. Restrictions apply to the availability of these data, which were used under license for the current study, and thus they are not publicly available. Data are, however, available from the authors upon reasonable request and with permission of Tokyo Electric Power Company Holdings, Inc.

**Code availability**

No custom code was used in this study. Data analyses were performed using standard software and custom scripts for image processing, which are available from the corresponding author upon reasonable request.

ARTICLE IN PRESS

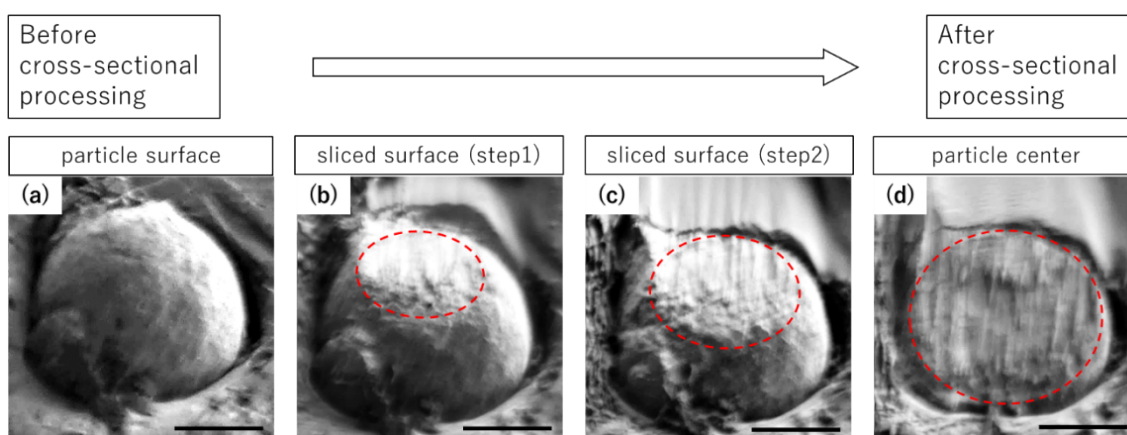
**Figures**

Fig. 1. Secondary electron image showing cross-sectional particle processing. The red dashed line indicates the FIB-sliced area. Scale bar: 20  $\mu\text{m}$

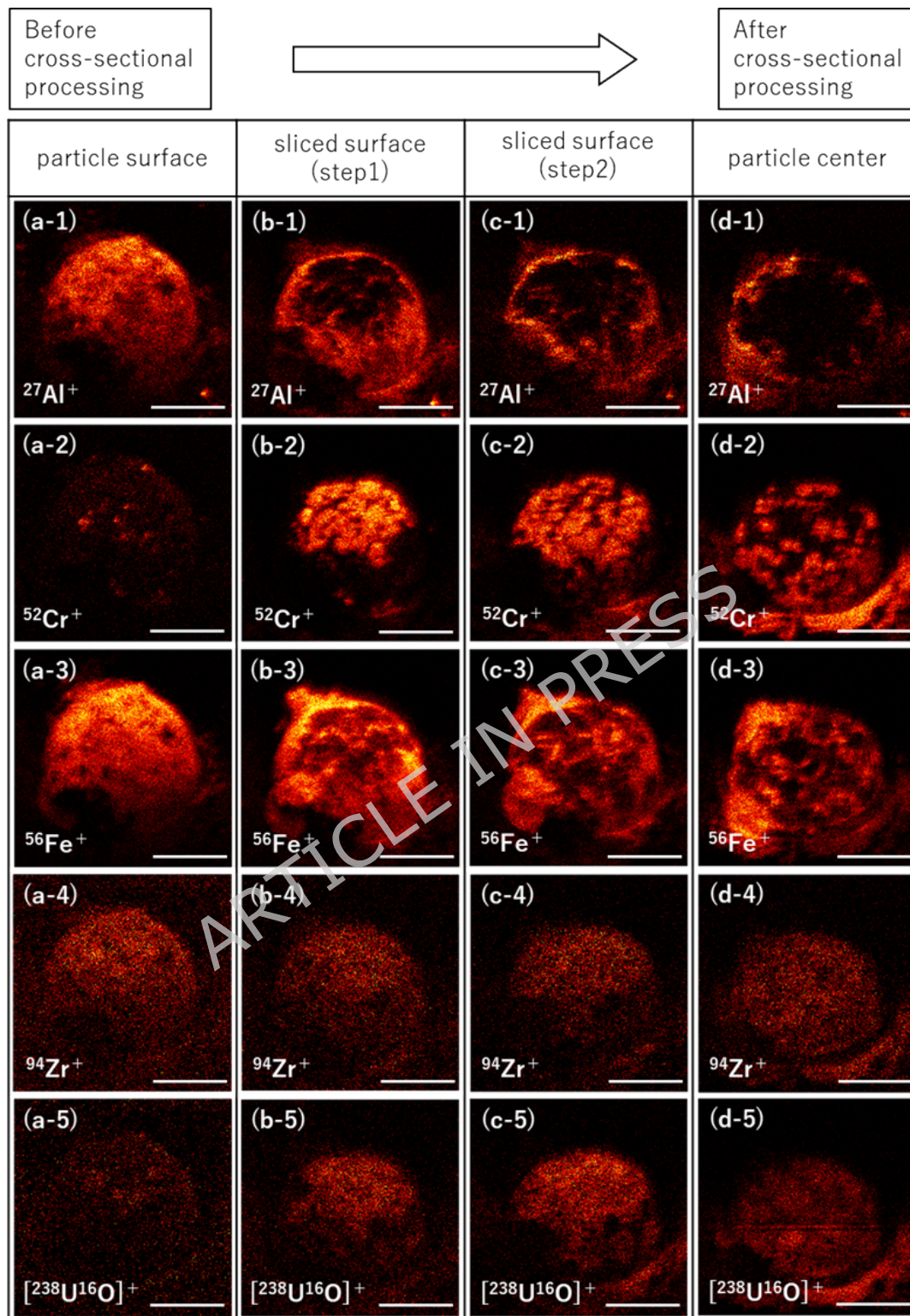


Fig. 2. SIMS compositional imaging results for each FIB-cut face (Fig. 1) showing the distributions of  $^{27}\text{Al}$ ,  $^{52}\text{Cr}$ ,  $^{94}\text{Zr}$ , and  $^{238}\text{U}^{16}\text{O}_2$ . Scale bar: 20  $\mu\text{m}$

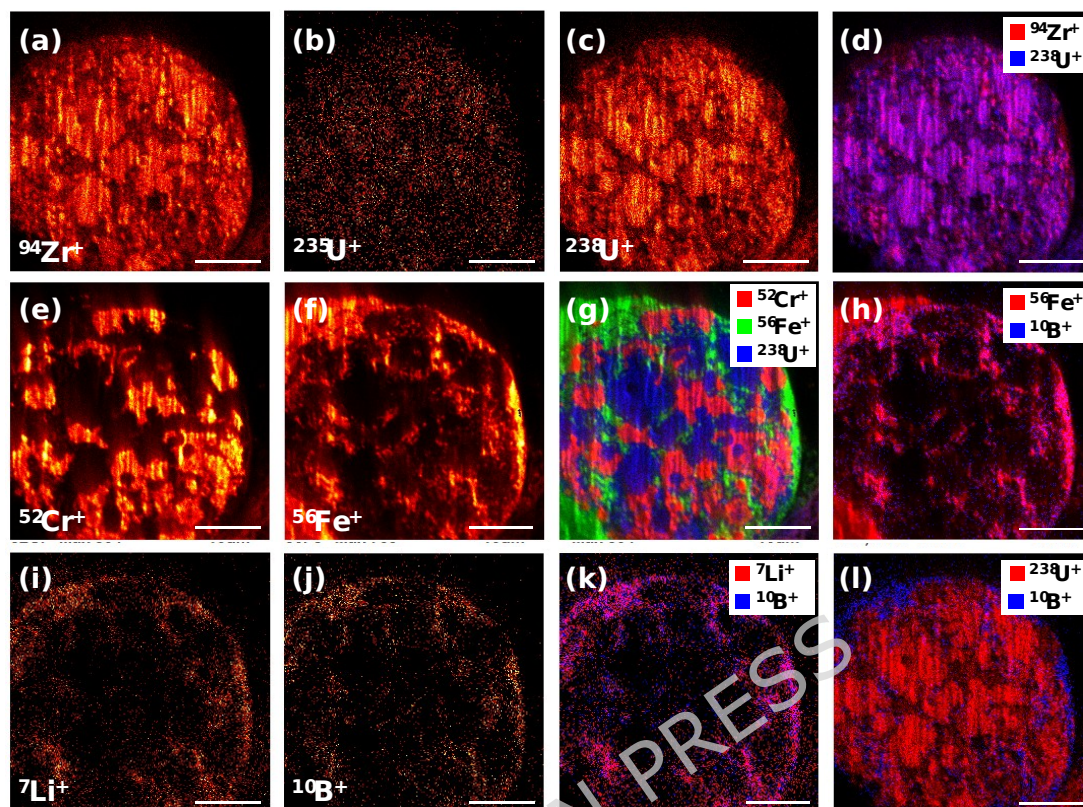


Fig. 3. High-resolution SIMS compositional imaging results for the FIB-cut face at the particle center (Fig. 1d), showing the distributions of  ${}^7\text{Li}$ ,  ${}^{10}\text{B}$ ,  ${}^{52}\text{Cr}$ ,  ${}^{56}\text{Fe}$ ,  ${}^{94}\text{Zr}$ ,  ${}^{235}\text{U}$ , and  ${}^{238}\text{U}$ . The purple regions in panels (d), (h), and (k) indicate areas where the red and blue color-coded element distributions overlap. Scale bar: 10  $\mu\text{m}$

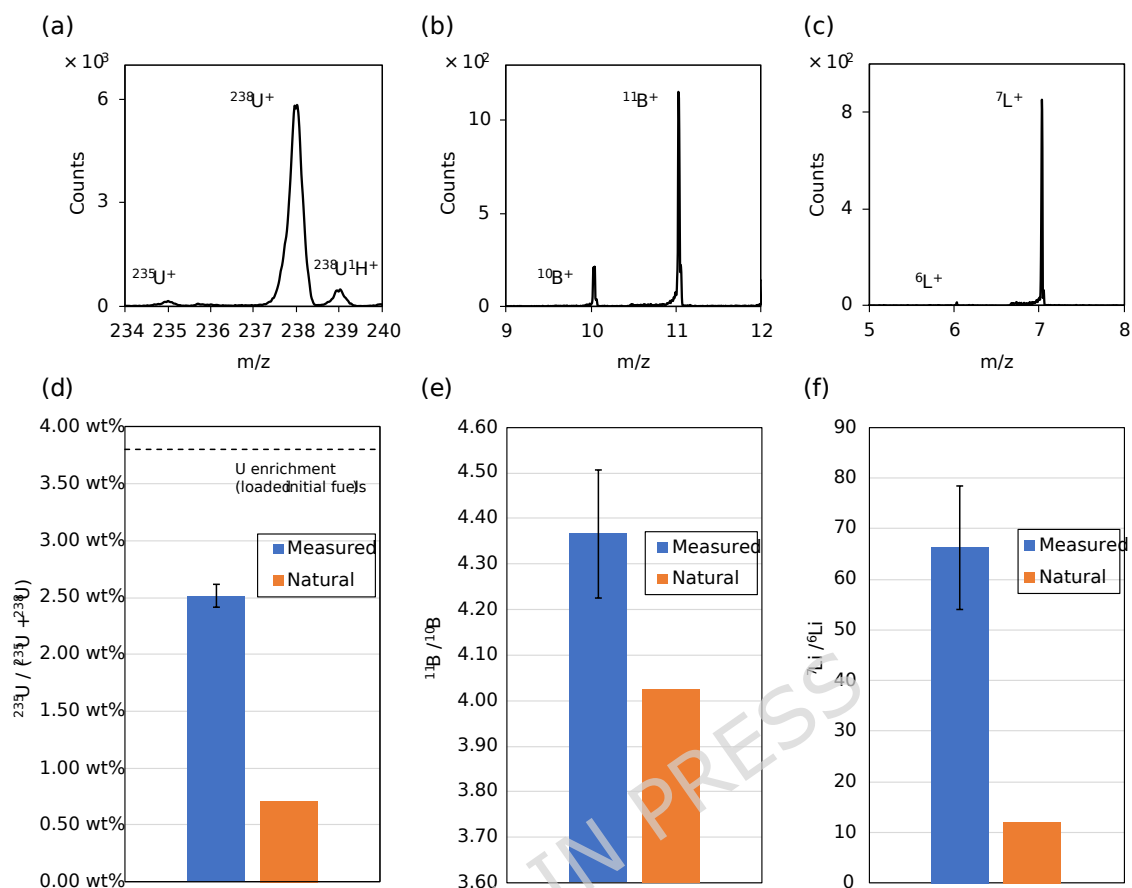


Fig. 4. (a-c): Representative SIMS mass spectra of U, B, and Li acquired from the cross-sectional region of the particle and used for isotope ratio evaluation. (d-f): Comparison of the U, B, and Li isotope ratios measured using SIMS (blue bars) with their natural isotope ratios (orange bars). The theoretical U isotope ratio at the time of initial fuel loading is shown as a dotted line in (d)<sup>18</sup>.